厚生労働科学研究費補助金

医療機器開発推進研究事業

固形がんの標的治療とその治療効果のMRIによる追跡を可能にする
診断-治療機能一体型DDSの創製

平成21年度　総括研究報告書

研究代表者　西山　伸宏

平成22（2010）年　5月

別紙1

厚生労働科学研究費補助金

医療機器開発推進研究事業

固形がんの標的治療とその治療効果のMRIによる追跡を可能にする
診断−治療機能一体型DDSの創製

平成２１年度　総括研究報告書

研究代表者　西山　伸宏

平成２２（２０１０）年　５月

別紙2

目　次

別紙3

厚生労働科学研究費補助金（医療機器開発推進研究事業）
総括研究報告書

固形がんの標的治療とその治療効果のMRIによる追跡を可能にする
診断-治療機能一体型DDSの創製

研究代表者　西山伸宏　東京大学大学院医学系研究科臨床医工学部門　准教授

研究要旨
がん組織に選択的に集積し、がんのMRI診断に広く利用できるMRI造影剤が望まれているが、そのような造影剤は未だ開発されていないのが現状である。また、がん化学療法においては、その有効性を的確に把握する必要があり、その目的においてMRIは有効な手段であると考えられる。そこで本研究では、現在、第一相臨床治験中のDachPt内包高分子ミセルに、MRI造影剤のGd-DTPAを搭載し、DachPtによる治療効果をMRIによって追跡できる診断-治療機能一体型DDSを開発することを目指している。本年度は、DachPt/Gd-DTPA内包ミセルの調製を行い、その物性評価ならびにMRI造影剤としての性能評価を行う一方で、マウス大腸がんモデルマウスを用いて、体内動態評価、制がん活性評価、がん組織のMRイメージングの検討を行った。

A．研究目的

　がん組織に選択的に集積し、がんのMRI診断に広く利用できるMRI造影剤が望まれているが、そのような造影剤は未だ開発されていないのが現状である。また、がん化学療法においては、その有効性を的確に把握する必要があり、その目的においてMRIは有効な手段であると考えられる。そこで本研究では、研究代表者である西山が過去に開発を行い、現在、第一相臨床治験中のオキサリプラチン活性体（DachPt）を内包する高分子ミセルに、MRI造影剤のGd-DTPAを搭載し、DachPtによる治療効果をMRIによって追跡できる診断-治療機能一体型DDSを開発することを目指している（図1）。近年、GdのデリバリーのためのDDSが活発に開発されているが、固形がんの選択的造影に成功した例は数少なく、すべてのシステムにおいてGdがDDS担体に安定な共有結合で導入されている為に、Gdの蓄積毒性が問題となるが、本研究では、Gd-DTPAとDachPtが可逆的な錯体を形成することを利用している為に、Gd-DTPAがDDS担体から最終的には放出され、安全性面において極めて優れている。さらに、本システムは、EPR効果によってがん組織での長期滞留が期待でき、術中MRIにおける位置把握精度向上のための強力なツールとなりうる。

　初年度にあたる平成21年度は、研究分担者であるCabralがDachPt/Gd-DTPA内包ミセルの調製を行い、その物性評価ならびにMRI造影剤としての性能評価を行う一方で、研究代表者である西山は、DachPt/Gd-DTPA内包ミセルのマウス大腸がんモデルマウスを用いて、体内動態評価、制がん活性評価、がん組織のMRイメージングの検討を行った。
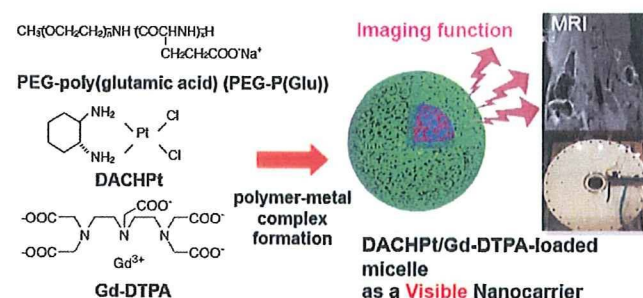

図1．診断-治療機能一体型DDSとしてのDachPt/Gd-DTPA内包ミセル

B．研究方法

1.DachPt/Gd-DTPA内包ミセルの調製

　5mMのDACHPt ジニトラト錯体と5mMのGd-DTPAを混合し、24時間培養した後、poly(ethylene glycol)-b-poly(glutamic acid) (PEG-b-P(Glu))ブロック共重合体（組成：PEG=12,000；P(Glu)重合度20）を[DACHPt]/[Glu]比が1になるように加え、120時間反応させた。その後、透析を行い、限外ろ過による精製を行った。DACHPt/Gd-DTPA内包ミセルの形成の有無は、動的光散乱(DLS)測定によって確認を行い、DACHPtおよびGd-DTPAの内包量はICP-MSにより定量した。また、DachPt/Gd-DTPA内包ミセルの安定性に関しては、150mM NaCl含有10mMリン酸緩衝液(pH7.4)中におけるミセルからのDACHPtおよびGd-DTPAの放出とミセルの散乱光強度の変化を測定した。さらに、DACHPt/Gd-DTPA

1

内包ミセルのT1緩和能をパルスNMRを用いたファントム実験により評価した。

2. DachPt/Gd-DTPA内包ミセルの体内動態評価

マウス大腸がんC-26細胞を皮下に移植したBalb/cマウス(♀, 6週齢)に対して、オキサリプラチン、Gd-DTPA、DachPt/Gd-DTPA内包ミセルを投与し、1、4、8、24時間後の血液中およびがん組織中のPtおよびGd量を組織の硝酸加熱後、ICP-MS測定を行うことにより定量した。

3. DachPt/Gd-DTPA内包ミセルの制がん活性評価

C-26皮下移植マウスに対して、1日おきに3回、オキサリプラチン(3mg/kg)およびDachPt/Gd-DTPA内包ミセル(8mg/kg)を投与し、経時的に腫瘍体積を測定することによって制がん活性を評価した。また、毒性を評価するために、マウスの体重変化の測定を同時に行った。

4. DachPt/Gd-DTPA内包ミセルによる固形がんのMRイメージング

C-26皮下移植マウスにGd-DTPAおよびDachPt/Gd-DTPA内包ミセルを投与し、4.7-T UNITY INOVA imaging spectrometer (Varian, Inc.)によって腫瘍のMRイメージングを行った。MRイメージングに関しては、ファントムをリファレンスとして投与から10分毎に4時間までの画像を取得した。

C. 研究結果

1. DachPt/Gd-DTPA内包ミセルの調製

DACHPtとGd-DTPAを異なる比率で混合し、PEG-b-P(Glu)と反応させることによって、DACHPt/Gd-DTPA内包ミセルの調製条件の最適化を行った。その結果、Gd-DTPAが5mMの条件において、DACHPtとGd-DTPAの両者が最も効率的に内包され、粒径33nmで非常に粒径分布の狭いナノ粒子の形成が確認された。ミセルに内包されたGd-DTPA量は、モル比でDACHPtの1/5であった。また、150mM NaCl含有10mMリン酸緩衝液(pH7.4)中におけるミセルからのDACHPtおよびGd-DTPAの放出を評価したところ、DACHPtとGd-DTPAは共にミセルから徐放されることが明らかとなり、24時間後におけるDACHPtおよびGd-DTPAのリリース量はそれぞれ10%および50%であった。さらに、パルスNMRを用いたファントム実験により、DACHPt/Gd-DTPA内包ミセルは、Gd-DTPAの24倍のT1緩和能を有することが明らかとなった。

2. DachPt/Gd-DTPA内包ミセルの体内動態評価

DachPt/Gd-DTPA内包ミセル投与後の血中のPtおよびGdの濃度を図2に示す。本結果では、DachPt/Gd-DTPA内包ミセルは、オキサリプラチンおよびGd-DTPAと比較してそれぞれ血中のPt濃度およびGd濃度を飛躍的に高めることが明らかになった。次に、がん組織(C-26)におけるPtおよびGd

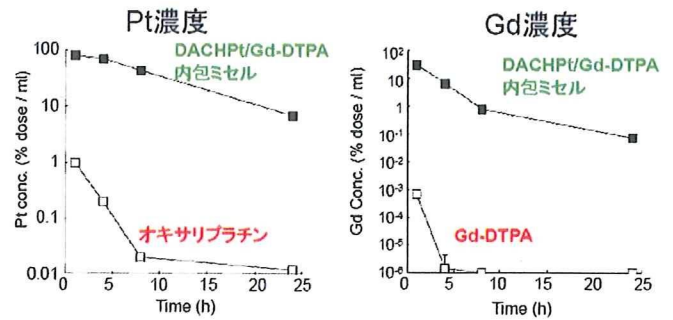の集積量を図3に示す。本結果においてもDachPt/Gd-DTPA内包ミセルは、オキサリプラチンおよびGd-DTPAと比較して顕著に高いがん集積性を示すことが明らかになった。一方、他の臓器に関しては、

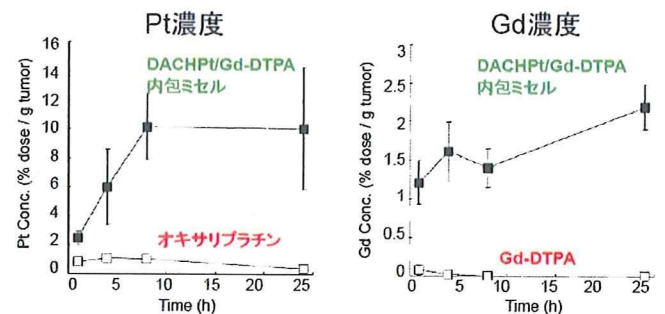図2. DachPt/Gd-DTPA内包ミセル、オキサリプラチンおよびGd-DTPAの全身投与後のPt(左)およびGd(右)の血中濃度

図3. DachPt/Gd-DTPA内包ミセル、オキサリプラチンおよびGd-DTPAの全身投与後のPt(左)およびGd(右)のがん集積性

3. DachPt/Gd-DTPA内包ミセルの制がん活性評価

DachPt/Gd-DTPA内包ミセルのC-26の皮下移植モデルに対する制がん活性を評価した結果を図4に示す。本結果では、オキサリプラチンは有意な制がん活性を示さなかったが、DachPt/Gd-DTPA内包ミセルは顕著に腫瘍の増殖を抑制することが明らかになった。
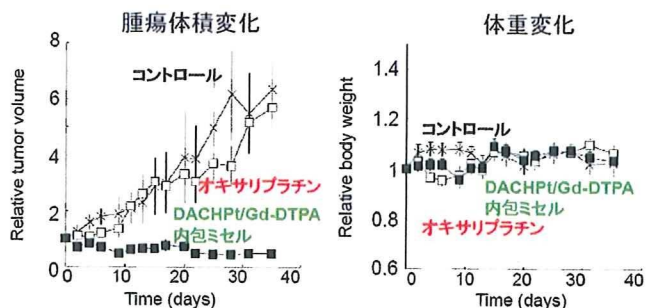

図4. DachPt/Gd-DTPA内包ミセルの制がん活性評価(左:相対腫瘍体積変化; 右:体重変化)

4. DachPt/Gd-DTPA内包ミセルによる固形がんのMRイメージング

DachPt/Gd-DTPA内包ミセルによる固形がん(C-26)のMRイメージングを行った(図5)。その結果、

Gd-DTPAの単独投与では腫瘍における明確なコントラストの増加は認められなかったが、DachPt/Gd-DTPA内包ミセルでは、顕著な固形がんの造影効果が確認され、2-6時間の長時間にわたり造影効果が維持されることが確認された。
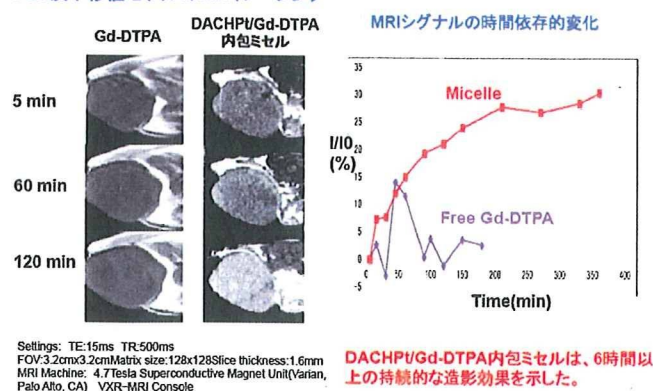
C-26皮下移植モデルのMRイメージング

図5．DachPt/Gd-DTPA内包ミセルによる固形がん（C-26モデル）のMRイメージング

D．考察

　本年度は、DachPtとGd-DTPAの混合比の最適化によって、33nmで粒径分布の狭いナノ粒子の形成が確認された。また、生理的条件下におけるミセルからのDACHPtおよびGd-DTPAのリリースを評価したところ、DACHPtとGd-DTPAは共にミセルから徐放されることが明らかとなり、Gd-DTPAはDACHPtよりも速くリリースすることが確認された。これは、制がん活性を示すDACHPtは、がん組織に滞留する必要がある一方で、Gd-DTPAはMRI撮像後になるべく速やかに体外に排泄されることが望ましいという点からは理想的な特性であると言える。一方で、MRI造影剤としての性能評価では、ミセルはGd-DTPAの24倍のT1緩和能を有することが確認され、MRI造影剤として非常に高い性能を有することが示唆された。次に、DachPt/Gd-DTPA内包ミセルの生物学的評価に関して、マウス大腸がん皮下移植モデルにおけるPtおよびGdのそれぞれの体内分布を評価したところ、優れた血中滞留性（24時間後のPtおよびGd血中濃度はそれぞれ20%および8%投与量／mL）と高い固形がん集積性（Ptの集積はオキサリプラチンの27倍、Gdの集積はGd-DTPAの100倍）が確認された（図2，4）。この結果は、ミセルのEPR効果による固形がんへの集積効果に基づくものと考えられる。また、DachPt/Gd-DTPA内包ミセルの固形がんに対する治療効果を検討した結果、オキサリプラチン単独よりも有意に高い制がん活性が確認された。この結果は、Gd-DTPAを添加しても現在臨床治験中のDACHPt内包ミセルの体内動態や制がん活性が維持されることを示唆している。さらに、DachPt/Gd-DTPA内包ミセルによるがん組織のMRイメージングに関しては、マウス大腸がん皮下移植

モデルにおいてGd-DTPAでは造影効果が確認されなかったが、ミセルにより腫瘍特異的なコントラストの増強が確認された。また、ミセルでは腫瘍におけるMRI信号強度の増大が6時間以上持続することが確認され、術中MRIの患部イメージングにも有用であることが示唆された。

E．結論

　本年度は、制がん剤DachPtとMRI造影剤Gd-DTPAを同時に搭載したDachPt/Gd-DTPA内包ミセルの調製法を確立した。DachPt/Gd-DTPA内包ミセルは、Gd-DTPAのT1緩和能を20倍以上に高める一方で、生理的条件下においてDachPtおよびGd-DTPAを徐放することが明らかになった。また、担がんマウスを用いた動物実験において、DachPt/Gd-DTPA内包ミセルは固形がんに選択的に集積し、強力ながん造影効果を示す一方で、優れた制がん活性を示すことが確認された。以上のように本システムは、DachPtによる治療効果をMRIによって追跡できる診断−治療機能一体型DDSとして今後の展開が期待される。

F．健康危険情報
本研究では現在のところ健康に危険を及ぼす可能性はない。

G．研究発表
1．論文発表
1. Y. Vachutinsky, M. Oba, K. Miyata, S. Hiki, M. R. Kano, N. Nishiyama, H. Koyama, K. Miyazono, K. Kataoka, Antiangiogenic gene therapy of experimental pancreatic tumor by sFlt-1 plasmid DNA carried by RGD-modified crosslinked polyplex micelles. *J. Control. Release*, in press

2. H. -J. Kim, A. Ishii, K. Miyata, Y. Lee, S. Wu, M. Oba, N. Nishiyama, K. Kataoka, Introduction of stearoyl moieties into a biocompatible cationic polyaspartamide derivative, PAsp(DET), with endosomal escaping function for enhanced siRNA-mediated gene knockdown. *J. Control. Release*, in press

3. K. Miyata, N. Gouda, H. Takemoto, M. Oba, Y. Lee, H. Koyama, Y. Yamasaki, K. Itaka, N. Nishiyama, K. Kataoka, Enhanced transfection with silica-coated polyplexes loading plasmid DNA. *Biomaterials* 31 (17) 4764-4770 (2010)

4. M. Oba, Y. Vachutinsky, K. Miyata, M. R. Kano, S. Ikeda, N. Nishiyama, K. Itaka, K. Miyazono, H. Koyama, K. Kataoka, Antiangiogenic gene therapy of solid tumor by systemic injection of polyplex micelles loading plasmid DNA encoding soluble Flt-1. *Mol. Pharm.*, 7 (2) 501-509 (2010)

5. H. Shimizu, Y. Hori, S. Kaname, K. Yamada, N. Nishiyama, S. Matsumoto, K. Miyata, M. Oba, A. Yamada, K. Kataoka, T. Fujita, siRNA-based therapy ameliorates glomerulonephritis. *J. Am. Soc. Nephrol.*, 21 (4) 622-633 (2010)

6. Y. Lee, T. Ishii, H. -J. Kim, N. Nishiyama, Y. Hayakawa, K. Itaka, K. Kataoka, Efficient delivery of bioactive antibodies into the cytoplasm of living cells by charge-conversional polyion complex micelles. *Angew. Chem. Int. Ed.*, 49 (14) 2552-2555 (2010)

7. K. Miyata, N. Gouda, H. Takemoto, M. Oba, Y. Lee, H. Koyama, Y. Yamasaki, K. Itaka, N. Nishiyama, K. Kataoka, Enhanced transfection with silica-coated polyplexes loading plasmid DNA. *Biomaterials*, 31 (17) 4764-4770 (2009)

8. M. Kumagai, M. R. Kano, Y. Morishita, M. Ota, Y. Imai, N. Nishiyama, M. Sekino, S. Ueno, K. Miyazono, K. Kataoka, Enhanced magnetic resonance imaging of experimental pancreatic tumor in vivo by block-copolymer-coated magnetite nanoparticles combined with TGF-beta inhibitor. *J. Control. Release*, 140 (3) 306-311 (2009)

9. M. Han, M. Oba, N. Nishiyama, M.R. Kano, S. Kizaka-Kondoh, K. Kataoka, Enhanced percolation and gene expression in tumor hypoxia by PEGylated polyplex micelles. **Mol. Ther.**, 17 (8) 1404-1410 (2009)

10. M. Harada-Shiba, I. Takamisawa, K. Miyata, T. Ishii, N. Nishiyama, K. Itaka, K. Kangawa, F. Yoshihara, Y. Asada, K. Hatakeyama, N. Nagaya, K. Kataoka, Intratracheal gene transfer of adrenomedullin using polyplex nanomicelles attenuates monocrotaline-induced pulmonary hypertension in rats. *Mol. Ther.*, 17 (7) 1180-1186 (2009)

11. M. Zhang, A. Ishii, N. Nishiyama, S. Matsumoto, T. Ishii, Y. Yamasaki, K. Kataoka, PEGylated calcium phosphate nanocomposites as smart environment-sensitive carriers for siRNA delivery. *Adv. Mater.* 21 (34) 3520-3525 (2009)

12. Y. Lee, T. Ishii, H. Cabral, H. -J. Kim, J. -H. Seo, N. Nishiyama, H. Oshima, K. Osada, K. Kataoka, Charge-conversional polyionic complex micelles-efficient nanocarriers for protein delivery into cytoplasm. *Angew. Chem. Int. Ed.* 48 (29) 5309-5312 (2009)

13. N. Nishiyama, Y. Morimoto, W.-D. Jang, K. Kataoka, Design and development of dendrimer photosensitizer-incorporated polymeric micelles for enhanced photodynamic therapy. *Adv. Drug Deliv. Rev.*, 61 (4) 327-338 (2009)

14. W. Wang, K. Itaka, S. Ohba, N. Nishiyama, U. Chung, Y. Yamasaki, K. Kataoka, Improving multipotent differentiation efficiency of mesenchymal stem cells using 3D spheroids method on micropatterned substrates. *Biomaterials*, 30 (14) 2705-2715 (2009)

15. S. Matsumoto, R. J. Christie, N. Nishiyama, K. Miyata, A. Ishii, M. Oba, H. Koyama, Y. Yamasaki, K. Kataoka, Environment-responsive block copolymer micelles with a disulfide cross-linked core for enhanced siRNA delivery. *Biomacromolecules*, 10 (1) 119-127 (2009)

16. N. Nishiyama, Y. Nakagishi, Y. Morimoto, P.-S. Lai, K. Miyazaki, K. Urano, S. Horie, M. Kumagai, S. Fukushima, Y. Cheng, W.-D. Jang, M. Kikuchi, K. Kataoka, Enhanced photodynamic cancer treatment by supramolecular nanocarriers charged with dendrimer phthalocyanine. *J. Control. Release* 133 (3) 245-251 (2009)

17. H. Cabral, M. Nakanishi, M. Kumagai, W.-D. Jang, N. Nishiyama, K. Kataoka, A photo-activated targeting chemotherapy using glutathione sensitive camptothecin-loaded polymeric micelles. *Pharm. Res.* 26 (1) 82-92 (2009)

2. 学会発表

1. 西山伸宏, "高分子ミセルを利用した診断・治療システムの開発", 第 48 回日本生体医工学会大会 オーガナイズドセッション 「ナノキャリアーと物理エネルギーを融合したハイブリット標的化診断・治療」, タワーホール船堀, 東京 2009 年 4 月 25 日 (シンポジスト)

2. 西山伸宏, 片岡一則 "がん標的治療のための高分子ミセル型 DDS の開発", 岡山肝癌研究会, 岡山コンベンションセンター, 岡山 2009 年 4 月 25 日(特別講演)

3. 西山伸宏, 熊谷康顕, 堀江壮太, 福島重人, 宮崎幸造, 浦野京子, 守本祐司, 張祐銅,片岡一則, "微小がんの光線力学治療のための診断-治療機能一体型高分子ミセルの開発", 第 58 回高分子学会年次会, 神戸国際会議場・神戸国際展示場, 神戸 2009 年 5 月 27-29 日(予定)

4. N. Nishiyama, "Block copolymer micelles as smart supramolecular nanodevices for tumor targeting", The 36th Annual Meeting and Exposition of the Controlled Release Society, Bella Center, Copenhagen Denmark, July 19, 2009 (Invited Lecture)

5. N. Nishiyama, Y. Morimoto, K. Miyazaki, K. Urano, S. Horie, M. Kumagai, S. Fukushima, W.-D. Jang, K. Kataoka, "Development of dendirimer phthalocyanine-loaded polymeric micelles for diagnosis and treatment of microcarcinoma", The 36th Annual Meeting and Exposition of the Controlled Release Society, Bella Center, Copenhagen Denmark, July 22, 2009

6. 西山伸宏, "ナノ技術を利用した DDS", 第 2 回 富山ライフサイエンスシンポジウム, 高志会館 「カルチャーホール」, 富山 2009 年 7 月 25 日(招待講演)

7. 西山伸宏, "高分子ミセル型医薬品の開発", 技術情

報協会セミナー　難治性がん治療薬開発に向けた治療の現状・DDS技術・マーカー開発, 大井町きゅりあん, 東京 2009年7月31日(招待講演)

8. <u>西山伸宏</u>, 韓ムリ, 大庭誠, カブラル・オラシオ, 狩野光伸, 片岡一則 "がん深部への遺伝子・薬剤デリバリーのためのナノキャリアの設計", 第58回高分子討論会, 熊本大学　黒髪キャンパス, 熊本 2009年9月17日(口頭)

9. <u>西山伸宏</u> "Development of polymeric micelles for innovative cancer therapy", 第68回 日本癌学会　シンポジウム「ナノテクノロジーがもたらす新規がん治療」, パシフィコ横浜, 神奈川 2009年10月2日(招待講演)

10. <u>西山伸宏</u>　"ナノテクノロジーが拓く未来医療", 現代科学セミナー, 東京理科大学長万部キャンパス, 北海道 2009年10月30日(招待講演)

11. <u>西山伸宏</u>, 片岡一則　"全身投与による遺伝子デリバリーのための高分子ナノキャリア設計", JST新技術説明会、JST東京本部, 東京 2009年11月20日(依頼講演)

12. <u>西山伸宏</u>, 宮田完二郎, 位高啓史, 大庭誠, 石井武彦, 片岡一則 "高機能ポリマー材料を基盤とした遺伝子デリバリーシステムの設計" 第18回ポリマー材料フォーラム研究会, タワーホール船堀, 東京 2009年11月24日(ポスター)

13. <u>西山伸宏</u>, "高分子集合体を基盤とした診断-治療一体型 DDS", 第3回 NEDO特別講座シンポジウム「次世代DDSが切り拓く未来医療」, 東京女子医科大学　弥生講堂, 東京 2009年12月12日(特別講義)

14. <u>西山伸宏</u>, "光線力学治療のための光増感剤内包高分子ミセルの開発", 日本薬学会第130年会 シンポジウム「異分野技術の融合による次世代の医療基盤技術の構築に向けて」, ホテルグランヴィア, 岡山 2010年3月29日(招待講演)

H．知的財産権の出願・登録状況

1. <u>西山伸宏</u>、狩野光伸、Horacio Cabral、片岡一則、Size Controlled Micelle of Plutinum Coordination Complex、米国仮出願　61/225716 (2009.7.15)

別紙4

厚生労働科学研究費補助金（医療機器開発推進研究事業）
分担研究報告書

固形がんの標的治療とその治療効果のMRIによる追跡を可能にする
診断-治療機能一体型DDSの創製
（DACHPt/Gd-DTPA内包ミセルの調製と緩和能の評価）

分担研究者　Cabral Horacio　東京大学大学院工学系研究科バイオエンジニアリング専攻
特任講師

研究要旨

本研究では、現在臨床治験中のDACHPt内包ミセルにMRI造影剤のGd-DTPAを搭載することによって、DACHPtによる治療効果をMRIによって追跡できる診断-機能一体型DDSの開発を行っている。本年度は、DACHPt/Gd-DTPA内包ミセルの調製条件の最適化を行い、生理的条件下におけるミセルからのDACHPtおよびGd-DTPAのリリースならびにT1緩和能の測定を行った。

A．研究目的

　MRIは、がんの非侵襲的診断法として極めて重要であるが、精度向上の為にはMRI造影剤の開発が重要である。これまでにGd-DTPA(マグネビスト)および磁性微粒子がそれぞれ脳腫瘍および肝がんの画像診断に利用されているが、前者では脳腫瘍で血液-脳関門が一部破綻していること、後者では微粒子が肝臓のクッパー細胞に貪食されることを利用しており、上記以外の固形がんのMRI診断に応用することが困難である。従って、がん組織に選択的に集積し、がんのMRI診断に広く利用できるMRI造影剤が望まれているが、そのような造影剤は未だ開発されていないのが現状である。一方、我々は、高分子ミセルを利用したDDSの開発に従事し、オキサリプラチン活性体(DACHPt)等の金属錯体を内包したミセルの開発に世界で初めて成功した。我々は、白金制がん剤を内包したミセルが、血中を長期滞留し、腫瘍血管の透過性亢進と未発達なリンパ系に起因するEnhanced Permeability and Retention (EPR)効果によって固形がんへの選択的集積と高い治療効果を示すことを明らかにしており、それらのミセルは現在、臨床治験中である。そこで本研究では、Gd-DTPAが有する遊離カルボキシル基が白金と可逆的な金属錯体を形成することに着目し、Gd-DTPAとDACHPtを同時に内包した高分子ミセルを構築し、上記以外の大腸がんや膵がん等に対するDACHPtのデリバリーによるがん標的治療とGd-DTPAのデリバリーによる制がん効果の追跡を可能にする世界初の診断-治療一体型DDSの開発を目指している。

　本分担研究では、本年度において、DACHPt/Gd-DTPA内包ミセルの調製条件の最適化を行い、生理的条件下におけるミセルからのDACHPtおよびGd-DTPAのリリースならびにT1緩和能の測定を行った。

B．研究方法

1. DACHPt/Gd-DTPA内包ミセルの調製

　5mMのDACHPt ジニトラト錯体と1-5mMのGd-DTPAを混合し、24時間培養した後、poly(ethylene glycol)-b-poly(glutamic acid) (PEG-b-P(Glu))ブロック共重合体(組成：PEG=12,000；P(Glu)重合度20)を[DACHPt]/[Glu]比が1になるように加え、120時間反応させた。その後、透析を行い、限外ろ過による精製を行った。DACHPt/Gd-DTPA内包ミセルの形成の有無は、動的光散乱(DLS)測定によって確認を行い、DACHPtおよびGd-DTPAの内包量はICP-MSにより定量した。

2. DACHPt/Gd-DTPA内包ミセルの物性評価

　DACHPt/Gd-DTPA内包ミセルは、水中では安定であるが、Cl^-イオン存在下においてはカルボキシレートからクロロへの配位子交換反応が生起し、ミセルからDACHPtおよびGd-DTPAが放出される一方で、ミセル自身は解離するものと考えられる。そこで、本項目では、150mM NaCl含有10mMリン酸緩衝液(pH7.4)中におけるミセルからのDACHPtおよびGd-DTPAの放出とミセルの散乱光強度の変化を測定した。

3. DACHPt/Gd-DTPA内包ミセルのT1緩和能の測定

DACHPt/Gd-DTPA内包ミセルのT1緩和能をパルスNMRを用いたファントム実験により評価した。T1緩和能(R1)は以下の式より算出した。

$$1/T1 = 1/T1_0 + R1[Gd]$$

T1: スピン-格子緩和時間(縦緩和時間)

C．研究結果

1. DACHPt/Gd-DTPA内包ミセルの調製

研究方法に従って調製したサンプル溶液のDLS測定を行った結果、粒径33nmで非常に粒径分布の狭い(PDI=0.067の)DACHPt/Gd-DTPA内包ミセルの形成が確認された。DACHPtとGd-DTPAの混合比を検討した結果、Gd-DTPAが5mMの条件において、DACHPtとGd-DTPAの両者が最も効率的に内包され、ポリマー1mg当たり0.42mgのDACHPt(P(Glu)のカルボキシル基の45%), 0.04mgのGd-DTPA(P(Glu)のカルボキシル基の5%)が内包されていることが確認された。

2. DACHPt/Gd-DTPA内包ミセルの物性評価

150mM NaCl含有10mMリン酸緩衝液(pH7.4)中におけるミセルからのDACHPtおよびGd-DTPAの放出を評価した(図1)。その結果、Gd-DTPAはDACHPtよりも速いリリースを示し、24時間後におけるDACHPtおよびGd-DTPAのリリース量はそれぞれ10%および50%であった。一方、ミセルの散乱光強度を測定した結果、DACHPtおよびGd-DTPAのリリースに伴い、ミセルの散乱光強度も減少し、40時間後には初期の20%まで散乱光強度が減少した。一方、DLS測定においては、ミセルの粒径に変化は見られず、24時間後においても初期の40nmの粒径が維持されることが確認された。
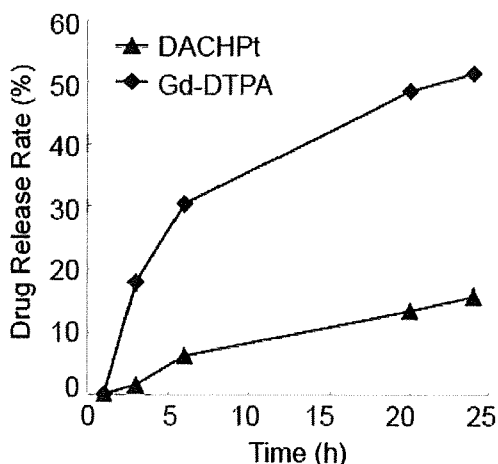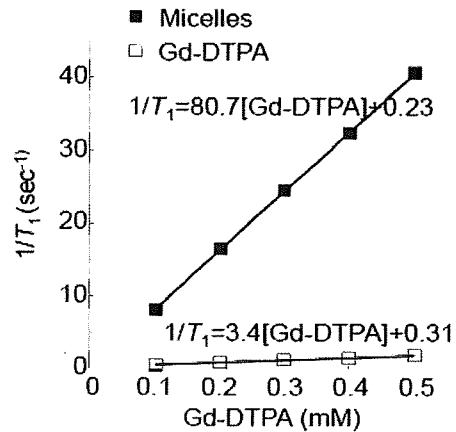
図1．150mM NaCl含有10mMリン酸緩衝液(pH7.4)中におけるミセルからのDACHPtおよびGd-DTPAの放出

3. DACHPt/Gd-DTPA内包ミセルのT1緩和能の測定

DACHPt/Gd-DTPA内包ミセルのT1緩和能をパルスNMRを用いたファントム実験により評価し

た。その結果、 DACHPt/Gd-DTPA内包ミセルは、Gd-DTPAの24倍のT1緩和能を有することが明らかとなった。

$1/T_1 = 80.7[Gd-DTPA]+0.23$

$1/T_1 = 3.4[Gd-DTPA]+0.31$

D．考察

本分担研究では、第一に、DACHPtとGd-DTPAを異なる比率で混合し、PEG-*b*-P(Glu)と反応させることによって、DACHPt/Gd-DTPA内包ミセルの調製条件の最適化を行った。その結果、Gd-DTPAが5mMの条件において、DACHPtとGd-DTPAの両者が最も効率的に内包され、粒径33nmで非常に粒径分布の狭いナノ粒子の形成が確認された。ミセルに内包されたGd-DTPA量は、モル比でDACHPtの1/5であった。本システムの特長として、水中ではミセルは非常に安定であるが、Clイオン存在下においてはPtのカルボキシレートからクロロへの配位子交換反応が生起し、ミセルからDACHPtおよびGd-DTPAが放出されることが挙げられる。そこで実際に、150mM NaCl含有10mMリン酸緩衝液(pH7.4)中におけるミセルからのDACHPtおよびGd-DTPAの放出を評価したところ、DACHPtとGd-DTPAは共にミセルから徐放されることが明らかとなり、24時間後におけるDACHPtおよびGd-DTPAのリリース量はそれぞれ10%および50%であった。本システムでは、Gd-DTPAの血中滞留性の向上によるがん集積性の向上が期待できる一方で、最終的には既に承認されているGd-DTPAが再生されるために、体内へのGdの蓄積などの問題を回避できるものと考えられる。最後に、パルスNMRを用いたファントム実験により、DACHPt/Gd-DTPA内包ミセルは、Gd-DTPAの24倍のT1緩和能を有することが明らかとなった。この結果に関しては、原因は明らかではないが、ミセルへの内包によりGd-DTPAの造影剤としての性能が飛躍的に向上することを示唆しており、より少ない投与量でがんのMRイメージングが可能となるものと期待される。

E．結論

本分担研究では、制がん剤DACHPtとMRI造影剤Gd-DTPAを同時に搭載した高分子ミセルの調

製法を確立した。DACHPt/Gd-DTPA内包ミセルは、水中では安定であるが、生理的条件下においては、DACHPtとGd-DTPAは共にミセルから徐放されることが明らかとなった。T1緩和能(R1)の測定においては、DACHPt/Gd-DTPA内包ミセルは、Gd-DTPA単独の24倍のR1値を示した。以上の結果より、DACHPt/Gd-DTPA内包ミセルは、優れたR1緩和能を有する一方で、徐々にDACHPtとGd-DTPAを放出し、Gd等の蓄積毒性を回避することができるものと考えられ、有効性と安全性と兼ね備えた治療-診断一体化システムとして今後は更なる最適化と物性評価ならびに生物学的評価を進めていきたいと考えている。

G．研究発表
1．論文発表
1. <u>H. Cabral</u>, K. Kataoka, Multifunctional nanoassemblies of block copolymers for future cancer therapy. *Sci. Technol. Adv. Mater.*, in press
2. <u>H. Cabral</u>, M. Nakanishi, M. Kumagai, W.-D. Jang, N. Nishiyama, K. Kataoka, A photo-activated targeting chemotherapy using glutathione sensitive camptothecin-loaded polymeric micelles. *Pharm. Res.* 26 (1) 82-92 (2009)
3. H. Cabral, K. Kataoka, Multifunctional nanoassemblies of block copolymers for future cancer therapy. Sci. Technol. Adv. Mater. in press

H．知的財産権の出願・登録状況
1. <u>Horacio Cabral</u>、西山伸宏、狩野光伸、片岡一則、Size Controlled Micelle of Plutinum Coordination Complex、米国仮出願　61/225716 (2009.7.15)

別紙5

研究成果の刊行に関する一覧表

雑誌

発表者氏名	論文タイトル名	発表誌名	巻号	ページ	出版年
M. Oba, N. Nishiyama et al.	Antiangiogenic gene therapy of solid tumor by systemic injection of polyplex micelles loading plasmid DNA encoding soluble Flt-1.	Mol. Pharm.	7	501-509	2010
M. Kumagai, N. Nishiyama et al.	Enhanced magnetic resonance imaging of experimental pancreatic tumor in vivo by block-copolymer-coated magnetite nanoparticles with TGF-beta inhibitor.	J. Control. Release	140	306-311	2009
M. Han, N. Nishiyama et al.	Enhanced percolation and gene expression in tumor hypoxia by PEGylated polyplex micelles.	Mol. Ther.	17	1404-1410	2009
N. Nishiyama, et al.	Design and development of dendrimer photosensitizer-incorporated polymeric micelles for enhanced photodynamic therapy.	Adv. Drug Deliv. Rev.,	61	327-338	2009
N. Nishiyama, et al.	Kataoka, Enhanced photodynamic cancer treatment by supramolecular nanocarriers charged with dendrimer phthalocyanine.	J. Control. Release	133	245-251	2009
H. Cabral, N. Nishiyama, et al.	A photo-activated targeting chemotherapy using glutathione sensitive camptothecin-loaded polymeric micelles.	Pharm. Res.	26	82-92	2009
H. Cabral et al.	Multifunctional nanoassemblies of block copolymers for future cancer therapy.	Sci. Technol. Adv. Mater.		印刷中	2010

9

Antiangiogenic Gene Therapy of Solid Tumor by Systemic Injection of Polyplex Micelles Loading Plasmid DNA Encoding Soluble Flt-1

Makoto Oba,[†] Yelena Vachutinsky,[‡] Kanjiro Miyata,[§] Mitsunobu R. Kano,[∥,⊥]
Sorato Ikeda,[#] Nobuhiro Nishiyama,[*,§] Keiji Itaka,[§] Kohei Miyazono,[∥,⊥]
Hiroyuki Koyama,[†] and Kazunori Kataoka[*,‡,§,∥,#]

*Department of Clinical Vascular Regeneration, Graduate School of Medicine, The
University of Tokyo, 7-3-1 Hongo, Bunkyo, Tokyo 113-8655, Japan, Department of
Bioengineering, Graduate School of Engineering, The University of Tokyo, 7-3-1 Hongo,
Bunkyo, Tokyo 113-8656, Japan, Center for Disease Biology and Integrative Medicine,
Graduate School of Medicine, The University of Tokyo, 7-3-1 Hongo, Bunkyo,
Tokyo 113-0033, Japan, Center for NanoBio Integration, The University of Tokyo, 7-3-1
Hongo, Bunkyo, Tokyo 113-8656, Japan, Department of Molecular Pathology, Graduate
School of Medicine, The University of Tokyo, 7-3-1 Hongo, Bunkyo-ku,
Tokyo 113-8655, Japan, and Department of Materials Engineering, Graduate School of
Engineering, The University of Tokyo, 7-3-1 Hongo, Bunkyo, Tokyo 113-8656, Japan*

Abstract: In this study, a polyplex micelle was developed as a potential formulation for antiangiogenic gene therapy of subcutaneous pancreatic tumor model. Poly(ethylene glycol)-poly(L-lysine) block copolymers (PEG-PLys) with thiol groups in the side chain of the PLys segment were synthesized and applied for preparation of disulfide cross-linked polyplex micelles through ion complexation with plasmid DNA (pDNA) encoding the soluble form of vascular endothelial growth factor (VEGF) receptor-1 (sFlt-1), which is a potent antiangiogenic molecule. Antitumor activity and gene expression of polyplex micelles with various cross-linking rates were evaluated in mice bearing subcutaneously xenografted BxPC3 cell line, derived from human pancreatic adenocarcinoma, and polyplex micelles with optimal cross-linking rate achieved effective suppression of tumor growth. Significant gene expression of this micelle was detected selectively in tumor tissue, and its antiangiogenic effect was confirmed by decreased vascular density inside the tumor. Therefore, the disulfide cross-linked polyplex micelle loading sFlt-1 pDNA has a great potential for antiangiogenic therapy against subcutaneous pancreatic tumor model by systemic application.

Keywords: Polymeric micelle; block copolymer; antiangiogenic tumor gene therapy; sFlt-1

Introduction

Antiangiogenic tumor gene therapy is an intensively studied approach to inhibit tumor growth by destructing its

neo-vasculature formation.[1,2] Vascular endothelial growth factor (VEGF) is a major proangiogenic molecule, which stimulates angiogenesis via promoting endothelial prolifera-

---

* To whom correspondence should be addressed. K.K.: tel, +81-3-5841-7138; fax, +81-3-5841-7139; e-mail, kataoka@bmw.t.u-tokyo.ac.jp; The University of Tokyo, Department of Materials Engineering, 7-3-1 Hongo, Bunkyo-ku, Tokyo 113-8656, Japan. N.N.: tel, +81-3-5841-1430; fax, +81-5841-7139; e-mail, nishiyama@bmw.t.u-tokyo.ac.jp.
† Department of Clinical Vascular Regeneration, Graduate School of Medicine.

‡ Department of Bioengineering, Graduate School of Engineering.
§ Center for Disease Biology and Integrative Medicine, Graduate School of Medicine.
∥ Center for NanoBio Integration.
⊥ Department of Molecular Pathology, Graduate School of Medicine.
Department of Materials Engineering, Graduate School of Engineering.

tion, survival, and migration. The soluble form of VEGF receptor-1 (fms-like tyrosine kinase-1: Flt-1) is a potent endogeneous molecule, which can be used for antiangiogenic therapy.[3,4] The sFlt-1 binds to VEGF with the same affinity and equivalent specificity as that of the original receptor,[5] however it inhibits its signal transduction.

Gene therapy is becoming a promising strategy to supply consecutive expression of antiangiogenic proteins over a period of time. Indeed, a number of studies have already demonstrated the potential of therapeutic genes encoding angiogenic inhibitors to suppress tumor growth.[6,7] The major challenge in systemic gene therapy, however, is a need for a safe and effective vector system that can deliver the gene to the target tissue and cells with no detrimental side effects. In terms of safety, nonviral gene vectors are gaining popularity over viral vectors, however, their intracellular delivery and transfection potential require further optimization. Recently, several reports were published on *in vivo* nonviral gene therapy utilizing sFlt-1 for inhibition of tumor angiogenesis.[8,9]

Based on these criteria, cross-linked polyplex micelles were designed and prepared through electrostatic interaction of thiolated poly(ethylene glycol)-poly(L-lysine) (PEG-PLys) block copolymers and plasmid DNA (pDNA) encoding sFlt-

1. We have previously reported that disulfide cross-links introduced into the polyplex micelle core contribute to the stabilization of its structure in the extracellular entity while facilitating smooth release of the entrapped pDNA, in response to the reductive environment, inside the cells.[10,11] The outer hydrophilic shell layer, formed by PEG segment, increases complex stability in serum, avoiding nonspecific interactions with plasma proteins and reduces polymer toxicity.[12]

In this study, cross-linked polyplex micelles were systemically administered to mice bearing subcutaneously xenografted BxPC3 human pancreatic adenocarcinoma and evaluated for their transfection efficiency. Note that BxPC3 xenografts, as some intractable solid tumors, are characterized by stroma-rich histology,[13] which limits access of therapeutic agents to tumor cells. Thus, the accessibility of endothelial cells by bloodstream makes an antiangiogenic approach an attractive strategy against this model. Here we report a potent tumor growth inhibitory effect achieved by effective antiangiogenic ability by the polyplex micelles with an optimal cross-linking degree, which enables the selective expression of loaded sFlt-1 gene in tumor tissue.

Experimental Section

Materials. pDNA for luciferase (Luc) with the pCAcc vector having the CAG promoter was provided by RIKEN Gene Bank (Tsukuba, Japan) and amplified in competent DH5α *Escherichia coli*, followed by purification using a NucleoBond Xtra Maxi (Machery-Nagel GmbH & Co. KG, Düren, Germany). Dulbecco's modified Eagle's medium (DMEM) and RPMI 1640 medium were purchased from Sigma-Aldrich Co. (Madison, WI). Fetal bovine serum (FBS) was purchased from Dainippon Sumitomo Pharma Co., Ltd. (Osaka, Japan). Alexa488- and Alexa647-conjugated secondary antibodies to rat IgG were obtained from Invitrogen Molecular Probes (Eugene, OR). Human soluble VEGF R1/

(1) Folkman, J. Tumor Angiogenesis: Therapeutic Implications. *N. Engl. J. Med.* **1971**, *285*, 1182–1186.

(2) Quesada, A. R.; Munoz-Chapuli, R.; Medina, M. A. Antiangiogenic Drugs: from Bench to Clinical Trials. *Med. Res. Rev.* **2006**, *26*, 483–530.

(3) Shibuya, M.; Yamaguchi, S.; Yamane, A.; Ikeda, T.; Tojo, A.; Matsushime, H.; Sato, M. Nucleotide Sequence and Expression of a Novel Human Receptor-type Tyrosine Kinase Gene (flt) Closely Related to the Fms Family. *Oncogene* **1990**, *5*, 519–524.

(4) Kendall, R. L.; Thomas, K. A. Inhibition of Vascular Endothelial Cell Growth Factor Activity by an Endogenously Encoded Soluble Receptor. *Proc. Natl. Acad. Sci. U.S.A.* **1993**, *90*, 10705–10709.

(5) Kendall, R. L.; Wang, G.; Thomas, K. A. Identification of a Natural Soluble Forma of the Vascular Endothelial Growth Factor Receptor, FLT-1, and Its Heterodimerization with KDR. *Biochem. Biophys. Res. Commun.* **1996**, *226*, 324–428.

(6) Kong, H. L.; Hecht, D.; Song, W.; Kovesdi, I.; Hackett, N. R.; Yayon, A.; Crystal, R. G. Regional Suppression of Tumor Growth by In Vivo Transfer of a cDNA Encoding a Secreted form of the Extracellular Domain of the Flt-1 Vascular Endothelial Growth Factor Receptor. *Hum. Gene Ther.* **1998**, *9*, 823–833.

(7) Kuo, C. J.; Farnebo, F.; Yu, E. Y.; Christofferson, R.; Swearingen, R. A.; Charter, R.; von Recum, H. A.; Yuan, J.; Kamihara, J.; Flynn, E.; D' Amato, R.; Folkman, J.; Mulligan, R. C. Comparative Evaluation of the Antitumor Activity of Antiangiogenic Proteins Delivered by Gene Transfer. *Proc. Natl. Acad. Sci. U.S.A.* **2001**, *98*, 4605–4610.

(8) Kim, W. J.; Yockman, J. W.; Jeong, J. H.; Christensen, L. V.; Lee, M.; Kim, Y. H.; Kim, S. W. Anti-angiogenic Inhibition of Tumor Growth by Systemic Delivery of PEI-g-PEG-RGD/pCMV-sFlt-1 Complexes in Tumor-bearing Mice. *J. Controlled Release* **2006**, *114*, 381–388.

(9) Kommareddy, S.; Amiji, M. Antiangiogenic Gene Therapy with Systemically Administered sFlt-1 Plasmid DNA in Engineered Gelatin-based Nanovactors. *Cancer Gene Ther.* **2007**, *14*, 488–498.

(10) Miyata, K.; Kakizawa, Y.; Nishiyama, N.; Harada, A.; Yamasaki, Y.; Koyama, H.; Kataoka, K. Block Catiomer Polyplexes with Regulated Densities of Charge and Disulfide Cross-linking Directed to Enhance Gene Expression. *J. Am. Chem. Soc.* **2004**, *126*, 2355–2361.

(11) Miyata, K.; Kakizawa, Y.; Nishiyama, N.; Yamasaki, Y.; Watanabe, T.; Kohara, M.; Kataoka, K. Freeze-dried Formulations for *In Vivo* Gene Delivery of PEGylated Polyplex Micelles with Disulfide Crosslinked Cores to the Liver. *J. Controlled Release* **2005**, *109*, 15–23.

(12) Itaka, K.; Yamauchi, K.; Harada, A.; Nakamura, K.; Kawaguchi, H.; Kataoka, K. Polyion Complex Micelles from Plasmid DNA and Poly(ethylene glycol)-poly(L-lysine) Block Copolymer as Serum-tolerable Polyplex System: Physicochemical Properties of Micelles Relevant to Gene Transfection Efficiency. *Biomaterials* **2003**, *24*, 4495–4506.

(13) Kano, M. R.; Bae, Y.; Iwata, K.; Morishita, Y.; Yashiro, M.; Oka, M.; Fujii, T.; Komuro, A.; Kiyono, K.; Kaminishi, M.; Hirakawa, K.; Ouchi, Y.; Nishiyama, N.; Kataoka, K.; Miyazono, K. Improvement of Cancer-targeting Therapy, Using Nanocarriers for Intractable Solid Tumors by Inhibition of TGF-beta Signaling. *Proc. Natl. Acad. Sci. U.S.A.* **2007**, *104*, 3460–3465.

Flt-1 immunoassay kit was purchased from R&D Systems, Inc. (Minneapolis, MN). Gemcitabine was obtained from Eli Lilly and Company (Indianapolis, IN). Avastin was obtained from F. Hoffmann-La Roche, Ltd. (Basel, Switzerland). Synthesis of thiolated block copolymer, and construction and confirmation of pDNA encoding sFlt-1 are shown in the Supporting Information. A block copolymer with $X\%$ of thiolation degree was abbreviated as "B-SH$X\%$".

Cell Lines and Animals. Human embryonic kidney 293T cells (from RIKEN CELL BANK, Tsukuba, Japan) and human pancreatic adenocarcinoma BxPC3 cells (from ATCC, Manassas, VA) were maintained in DMEM and RPMI medium, respectively, supplemented with 10% FBS in a humidified atmosphere containing 5% CO_2 at 37 °C. 293T cells were chosen for *in vitro* experiments as cells that did not express sFlt-1.[14] Balb/c nude mice (female, 5 weeks old) were purchased from Charles River Laboratories (Tokyo, Japan). All animal experimental protocols were performed in accordance with the Guide for the Care and Use of Laboratory Animals as stated by the National Institutes of Health.

Preparation of Polyplex Micelles. Each block copolymer was dissolved in 10 mM Tris-HCl buffer (pH 7.4), followed by the addition of 10-times-excess mol of dithiothreitol (DTT) against thiol groups. After 30 min incubation at room temperature, the polymer solution was added to a twice-excess volume of 225 μg/mL pDNA/10 mM Tris-HCl (pH 7.4) solution to form polyplex micelles with N/P ratio = 2. Note that N/P ratio was defined as the residual molar ratio of amino groups of thiolated PEG-PLys to phosphate groups of pDNA. The final pDNA concentration was adjusted to 150 μg/mL. After overnight incubation at room temperature, the polyplex micelle solution was dialyzed against 10 mM Tris-HCl buffer (pH 7.4) containing 0.5 vol% DMSO at 37 °C for 24 h to remove the impurities, followed by 24 h of additional dialysis against 10 mM Tris-HCl buffer (pH 7.4) or 10 mM Hepes buffer (pH 7.4) to remove DMSO. During the dialysis, the thiol groups of thiolated block copolymers were oxidized to form disulfide cross-links. In the *in vivo* experiments, the polyplex micelle solution was adjusted to a concentration of 100 μg of pDNA/mL in 10 mM Hepes buffer (pH 7.4) with 150 mM NaCl.

Dynamic Light Scattering (DLS) Measurement. The size of the polyplex micelles was evaluated by DLS using Nano ZS (ZEN3600, Malvern Instruments, Ltd., U.K.). A He—Ne ion laser (633 nm) was used as the incident beam. Polyplex micelle solutions with N/P = 2 from 3 different batches were adjusted to a concentration of 33.3 μg of pDNA/mL in 10 mM Tris-HCl buffer (pH 7.4). The data obtained at a detection angle of 173° and a temperature of 37 °C were analyzed by a cumulant method to obtain the hydrodynamic diameters and polydispersity indices (μ/Γ^2) of micelles.

Zeta-Potential Measurement. The zeta-potential of polyplex micelles was evaluated by the laser-Doppler electrophoresis method using Nano ZS with a He—Ne ion laser (633 nm). Polyplex micelle solutions with N/P = 2 from 3 different batches were adjusted to a concentration of 33.3 μg pDNA/mL in 10 mM Tris-HCl buffer (pH 7.4). The zeta-potential measurements were carried out at 37 °C. A scattering angle of 173 °C was used in these measurements.

Real-Time Gene Expression. 293T cells (100,000 cells) were seeded on a 35 mm dish and incubated overnight. After replacement with fresh medium containing 0.1 mM D-luciferin, each type of polyplex micelle (N/P = 2) containing 3 μg of Luc pDNA was added. The dishes were set in a luminometer incorporated in a CO_2 incubator (AB-2550 Kronos Dio, ATTO, Tokyo, Japan), and the bioluminescence was monitored every 10 min with an exposure time of 1 min. Reproducibility was confirmed by triplicate experiments.

Antitumor Activity Assay. Balb/c nude mice were inoculated subcutaneously with BxPC3 cells (5 × 10^6 cells in 100 μL of PBS). Tumors were allowed to grow for 2—3 weeks to reach the proliferative phase (the size of the tumors at this point was approximately 60 mm^3). Subsequently, polyplex micelles (20 μg of pDNA/mouse), gemcitabine (100 mg/kg), or Avastin (50 mg/kg) maintained in 10 mM Hepes buffer (pH 7.4) with 150 mM NaCl were injected via the tail vein either 3 times (Figure 2a) or 5 times (Figure 2b) at 4-day intervals. Gemcitabine and Avastin doses and injection regimens were according to the previous reports published elsewhere.[15,16] A polyplex micelle containing Luc pDNA was used as a control formulation containing the nontherapeutic gene. Tumor size was measured every second day by a digital vernier caliper across its longest (a) and shortest diameters (b), and its volume (V) was calculated according to the formula $V = 0.5ab^2$.

In Vivo **sFlt-1 Gene Expression.** Polyplex micelles loading either sFlt-1 or Luc pDNA (20 μg pDNA) were injected into the BxPC3-inoculated mice via the tail vein on days 0 and 4. Mice were sacrificed on day 6 after collecting blood, and the lungs, livers, spleens, kidneys, and tumors were excised. The excised organs were treated in 500 μL of cell culture lysis buffer (Promega, Madison, WI), homogenized, and centrifuged. The sFlt-1 concentration of supernatants was evaluated using the immunoassay kit according to the manufacturer's protocol. Note that block copolymers and polyplex micelles did not interfere with ELISA (Figure 2 in the Supporting Information).

Vascular Density in the Tumors. Polyplex micelles loading either sFlt-1 or Luc pDNA (20 μg of pDNA) and Avastin (50 mg/kg) were injected into the BxPC3-inoculated

(14) Kim, W. J.; Yockman, J. W.; Lee, M.; Jeong, J. H.; Kim, Y. H.; Kim, S. W. Soluble Flt-1 Gene Delivery Using PEI-g-PEG-RGD Conjugate for Anti-angiogenesis. *J. Controlled Release* **2005**, *106*, 224–234.

(15) Braakhuis, B. J. M.; van Dongen, G. A. M. S.; Vermorken, J. B.; Snow, G. B. Preclinical In Vivo Activity 2′,2′-Difluorodeoxycytidine (Gemcitabine) against Human Head and Neck Cancer. *Cancer Res.* **1991**, *51*, 211–214.

(16) Gerber, H. P.; Ferrara, N. Pharmacology and Pharmacodynamics of Bevacizumab as Monotherapy or in Combination with Cytotoxic Therapy in Preclinical Studies. *Cancer Res.* **2005**, *65*, 671–680.

mice via the tail vein on days 0 and 4. Mice were sacrificed on day 6, and the tumors were excised, frozen in dry-iced acetone, and sectioned at 10 μm thickness in a cryostat. Vascular endothelial cells (VECs) were immunostained by rat monoclonal antibody antiplatelet endothelial cell adhesion molecule-1 (PECAM-1) (BD Pharmingen, Franklin Lakes, NJ) and Alexa488-conjugated secondary antibody. The samples were observed with a confocal laser scanning microscope (CLSM). The CLSM observation was performed using an LSM 510 (Carl Zeiss, Oberlochen, Germany) with an EC Plan-Neoflur 20× objective (Carl Zeiss) at the excitation wavelength of 488 nm (Ar laser). The PECAM-1-positive area (%) was calculated from Alexa488-positive pixels.

***In Vivo* EGFP Gene Expression in the Tumors.** Polyplex micelles loading EGFP pDNA (20 μg of pDNA) were injected into the BxPC3-inoculated mice via the tail vein. Mice were sacrificed on either day 3 or day 7. Tumors were excised, fixed with 10% formalin, frozen, and sectioned. VECs were immunostained by anti-PECAM-1 antibody and Alexa647-conjugated secondary antibody. After nuclear staining with Hoechst 33342, CLSM observation was carried out using the LSM 510 with the EC Plan-Neoflur 20× objective at the excitation wavelength of 488 nm for EGFP expression, 633 nm (He−Ne laser) for Alexa647, and 710 nm (MaiTai laser, two photon excitation; Spectra-Physics, Mountain View, CA) for Hoechst 33342, respectively. The representative images of tumors excised on day 3 are shown in Figure 5. Note that images of tumors excised on day 7 showed similar patterns to those on day 3, however with lower intensity of EGFP expression.

Results

Formation of Polyplex Micelles. No free pDNA was detected by agarose gel electrophoresis, confirming that all pDNA was entrapped in disulfide cross-linked polyplex micelles, which were prepared as previously reported through ion complexation of block copolymers with pDNA at the N/P ratio = 2. Free thiol groups in polyplex micelles were estimated to be less than 2% by Ellman's test (data not shown), which is consistent with our previous report.[10] Weight−weight % ratios of pDNA/micelle in each formulation were as follows: 32.8% in B-SH0% formulation; 31.0% in B-SH5%; 29.2% in B-SH11%; 26.4% in B-SH20%; and 21.0% in B-SH36%. The mean size of the micelles was between 100 and 150 nm, with a moderate polydispersity index between 0.17 and 0.2 (Figure 3 in the Supporting Information), while zeta-potential revealed approximately neutral values, confirming the formation of PEG palisade surrounding the polyplex core (Table 1).

Real-Time Gene Expression. *In vitro* real-time Luc gene expression of polyplex micelles was evaluated using Kronos

Table 1. Sizes and Zeta-Potentials of Polyplex Micelles with Various Cross-Linking Rates at N/P = 2[a]

thiolation degree (%)	cumulant diameter (nm)	polydispersity index (μ/Γ^2)	zeta-potential (mV)
0	107 ± 2	0.195 ± 0.021	1.66 ± 0.28
5	117 ± 2	0.184 ± 0.011	1.25 ± 0.40
11	116 ± 2	0.171 ± 0.013	1.02 ± 0.30
20	139 ± 6	0.182 ± 0.050	0.40 ± 0.07
36	147 ± 2	0.192 ± 0.061	−0.96 ± 0.02

[a] The results reported were expressed as mean ± SEM (n = 3).
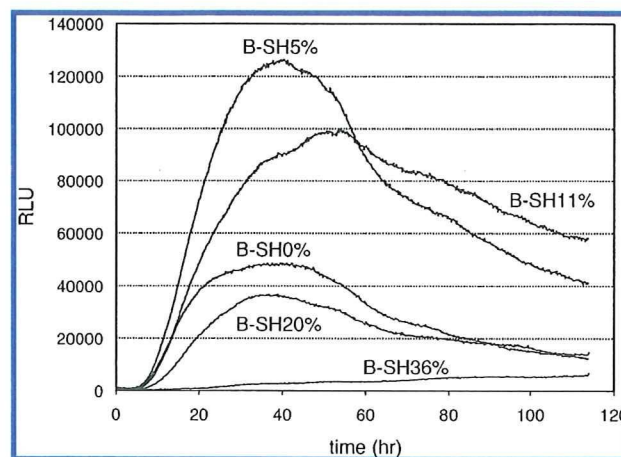

Figure 1. Real-time luciferase gene expression of the polyplex micelles with varying thiolation degrees at N/P = 2 against 293T cells.

Dio for a prolonged period (Figure 1).[17,18] The B-SH5% cross-linked polyplex micelle showed the highest gene expression among all micelles until 60 h. Worth mentioning is that the transfection efficiency of the B-SH11% micelle continued to exceed that of the B-SH5% micelle after 60 h. Disulfide cross-links in the polyplex core are believed to contribute not only to enhanced stability of the micelles in the medium but also to sustained release of complexed pDNA inside the cells with a reductive environment, resulting in polyplex micelles with higher cross-linking rates that can maintain an appreciable transfection efficiency over a longer time scale. Note that the B-SH36% micelle showed an increasing trend in gene expression with time.

Antitumor Activity. Polyplex micelles containing sFlt-1 pDNA were injected iv into mice bearing pancreatic adeno-carcinoma BxPC3, followed by evaluation of tumor volume (Figure 2). All the micelles were injected three times on days

(17) Takae, S.; Miyata, K.; Oba, M.; Ishii, T.; Nishiyama, N.; Itaka, K.; Yamasaki, Y.; Koyama, H.; Kataoka, K. PEG-detachable Polyplex Micelles Based on Disulfide-crosslinked Block Cationers as Bioresponsive Nonviral Gene Vectors. *J. Am. Chem. Soc.* **2008,** *130,* 6001–6009.

(18) Oba, M.; Aoyagi, K.; Miyata, K.; Matsumoto, Y.; Itaka, K.; Nishiyama, N.; Yamasaki, Y.; Koyama, H.; Kataoka, K. Polyplex Micelles with Cyclic RGD Peptide Ligands and Disulfide Cross-links Directing to the Enhanced Transfection via Controlled Intracellular Trafficking. *Mol. Pharmaceutics* **2008,** *5,* 1080–1092.
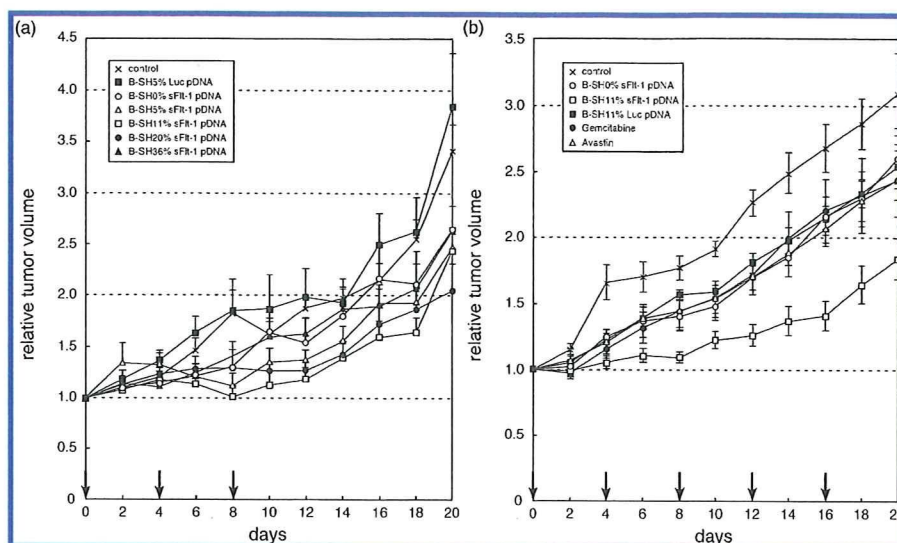
Figure 2. Antitumor activity of polyplex micelles with sFlt-1 pDNA in subcutaneously BxPC3-inoculated mice. (a) Effect of thiolation degree. Hepes buffer (control) was used as a negative control. Polyplex micelles were injected iv on days 0, 4, and 8 at 20 μg pDNA/mouse, and mice were monitored for the relative tumor volume every second day. Error bars represent the SEM ($n = 6$). Only the B-SH11% polyplex micelles exhibited significant retardation of tumor growth compared to the control ($P < 0.01$). (b) Growth curve study with an increased dose of the B-SH11% polyplex micelles compared to commercially available drugs. Polyplex micelles (20 μg pDNA/mouse), gemcitabine (100 mg/kg), and Avastin (50 mg/kg) were injected iv on days 0, 4, 8, 12, and 16. Relative tumor size was measured every second day. Hepes buffer (control) was used as a negative control. Error bars represent the SEM ($n = 5$). Only the B-SH11% polyplex micelles exhibited significant retardation of tumor growth compared to the control ($P < 0.001$). P values were calculated by multivariate ANOVA study.
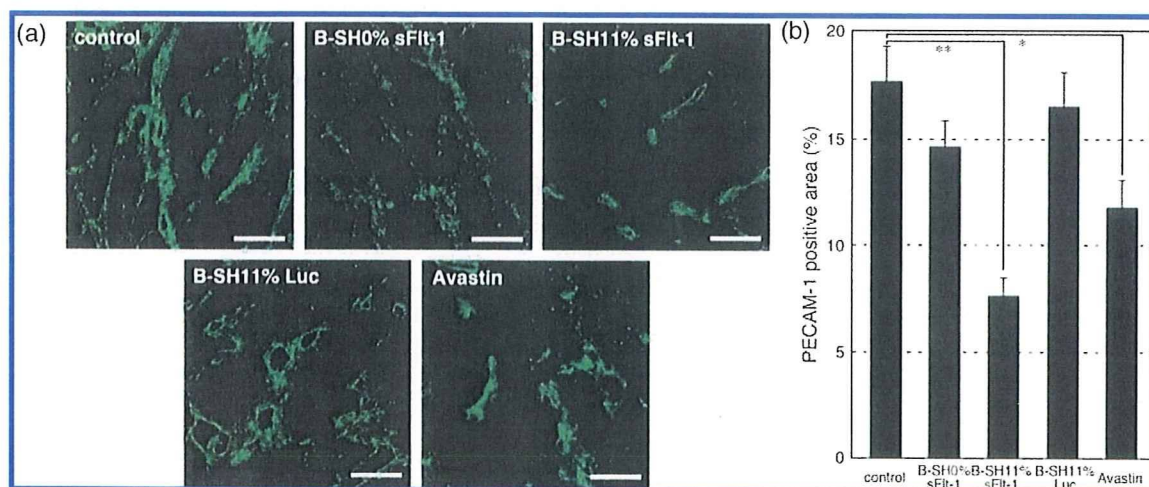
Figure 3. Immunostaining of the VECs in the BxPC3 tumor tissue by PECAM-1 antibody. Hepes buffer (control), three types of polyplex micelles (20 μg of pDNA/mouse), and Avastin (50 mg/kg) were injected into the BxPC3-inoculated mice via the tail vein on days 0 and 4. Mice were sacrificed on day 6, and tumors were excised and immunostained. (a) CLSM images of immunostained tumors. PECAM-1-positive regions are green. Bars represent 100 μm. (b) Areas of PECM-1-positive endothelium were quantified. Error bars represent the SEM ($n = 15$). P values were calculated by Student's t test. *$P < 0.01$ and **$P < 0.001$.

0, 4, and 8 (Figure 2a). The B-SH11% micelle significantly suppressed tumor growth compared to control mice treated with Hepes buffer ($P < 0.01$). There was no significant change in tumor growth after injection of other polyplex micelles, implying that an optimal cross-linking rate is required to achieve an effective expression of the gene. Encouraged by these results, the tumor growth suppression
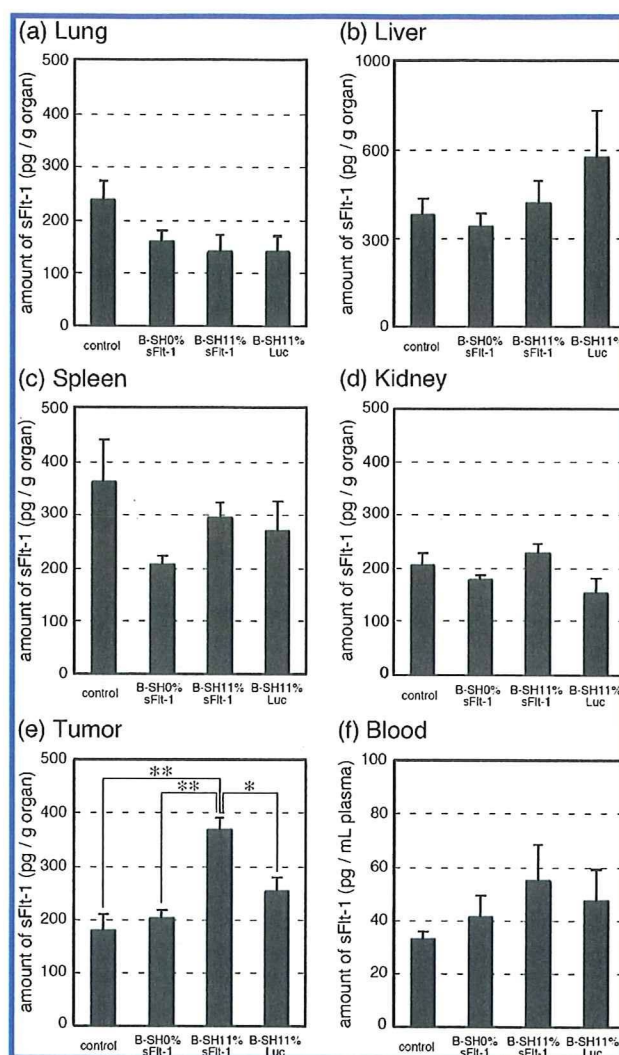
activity of B-SH11% micelle was further evaluated, implying a regimen with enhanced number of injections. The effect of the micelles was compared to commercially available drugs, gemcitabine, a standard chemotherapeutic agent for pancreatic tumor, and bevacizumab (Avastin), a monoclonal antibody against VEGF (Figure 2b). The doses of gemcitabine and Avastin implied in our study were based on

previous reports published elsewhere.[15,16] The administration of B-SH11%/sFlt-1 micelle resulted in significant suppression of tumor growth ($P < 0.001$), while gemcitabine and Avastin, under the reported experimental regimen, showed no remarkable therapeutic effect. Note that the difference observed in tumor volumes between the B-SH11%/Luc micelle-treated group and the control group was not significant.

Tumor Vascular Density. The antiangiogenic effect of expressed sFlt-1 was confirmed by immunostaining of VECs using PECAM-1 (Figure 3). Vascular density of tumors treated with either B-SH11%/sFlt-1 micelle or Avastin was significantly lower than that of the other groups. The most pronounced and significant effect on neo-vasculature suppression was achieved by B-SH11%/sFlt-1 micelle (7% PECAM-1 positive area) over Avastin (12% PECAM-1 positive area) ($P < 0.05$). These results suggest that the expressed sFlt-1 may entrap VEGF secreted in the tumor tissue, thereby suppressing the growth of VECs.

In Vivo **sFlt-1 Gene Expression.** Expression levels of sFlt-1 in the body were then evaluated by measuring the amount of sFlt-1 in lung, liver, spleen, kidney, tumor, and blood plasma using enzyme-linked immunosorbent assay (ELISA) (Figure 4). Injection of B-SH11%/sFlt-1 micelle resulted in significantly higher expression of sFlt-1 selectively in tumor tissue compared to the control. On the other hand, injection of B-SH0%/sFlt-1 micelle or B-SH11%/Luc micelle did not result in any difference in sFlt-1 expression compared to the control. These results strongly support that tumor-specific elevation in sFlt-1 expression led to the significant growth suppression of VECs in the tumor tissue and, eventually, the suppression of tumor growth.

In Vivo **Enhanced Green Fluorescence Protein (EGFP) Gene Expression in Tumors.** The location of gene expression in BxPC3 tumors after administration of the micelles was analyzed histologically using pDNA encoding EGFP (Figure 5). As previously reported,[13,19,20] thick fibrotic tissue was formed around blood vessels (red) inside the stroma of BxPC3 tumors, and nests of tumor cells (region T) were scattered in the stroma (Figure 5a). The expression of EGFP (Figures 5b and 5c) was observed mainly in the VECs and cells in stromal regions adjacent to some vasculature, indicating that VECs and fibroblasts near some vasculature in the stroma, but not the tumor cells, were transfected. As seen in Figure 5a, there were thick fibrotic tissues around blood vessels in the BxPC3 xenograft,
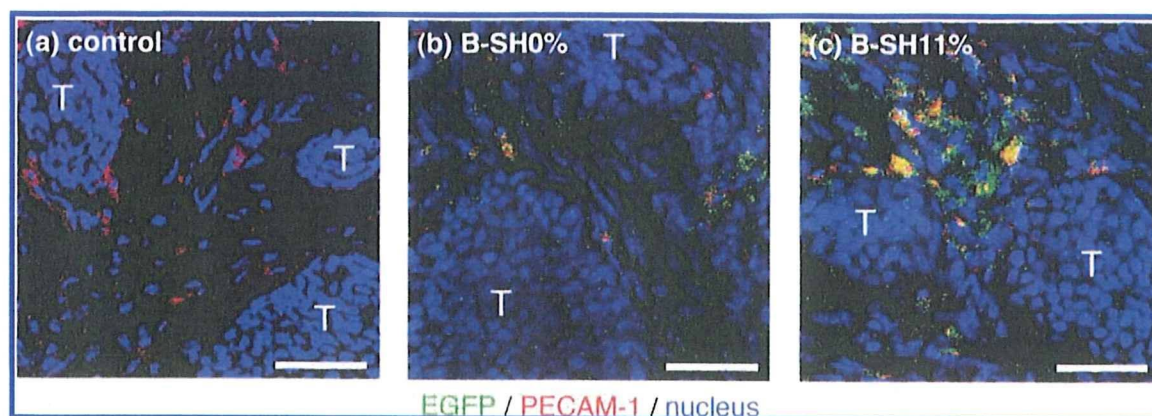
(19) Miyata, K.; Oba, M.; Kano, M. R.; Fukushima, S.; Vachutinsky, Y.; Han, M.; Koyama, H.; Miyazono, K.; Nishiyama, N.; Kataoka, K. Polyplex Micelles from Triblock Copolymers Composed of Tandemly Aligned Segments with Biocompatible, Endosomal Escaping, and DNA-condensing Functions for Systemic Gene Delivery to Pancreatic Tumor Tissue. *Pharm. Res.* **2008**, *25*, 2924–2936.

(20) Kano, M. R.; Komuta, Y.; Iwata, K.; Oka, M.; Shirai, Y.; Morishita, Y.; Ouchi, Y.; Kataoka, K.; Miyazono, K. Comparison of the Effects of the Kinase Inhibitors Imatinib, Sorafenib, and Transforming Growth Factor-β Receptor Inhibitor on Extravasation of Nanoparticles from Neovasculature. *Cancer Sci.* **2009**, *100*, 173–180.

Figure 4. Evaluation of sFlt-1 gene expression in organs by ELISA. Hepes buffer (control) and three types of polyplex micelles (20 µg pDNA/mouse) were injected into the BxPC3-inoculated mice via the tail vein on days 0 and 4. Mice were sacrificed on day 6 after collecting blood (f), and the lungs (a), livers (b), spleens (c), kidneys (d), and tumors (e) were excised, followed by evaluation of sFlt-1 concentration by ELISA according to the manufacturer's protocol. Error bars represent the SEM ($n = 6$). P values were calculated by Student's t test. $^*P < 0.01$ and $^{**}P < 0.001$.

indicating that the penetration of polyplex micelles deep into the stroma or into the tumor nest was interrupted and the gene expression was limited in the VECs and some of the fibroblasts in the stroma. Higher levels of EGFP expression were observed for B-SH11% micelle, confirming their enhanced ability to accumulate inside tumor tissue compared to B-SH0% micelle.

Discussion

Since all solid tumors need angiogenesis for their growth, antiangiogenic therapy is a promising strategy for treating

Figure 5. EGFP gene expression by polyplex micelles in the inoculated BxPC3 tumors. Hepes buffer (a) was used as a negative control. B-SH0% (b) and B-SH11% (c) polyplex micelles containing EGFP pDNA (20 μg pDNA/mouse) were injected into the BxPC3-inoculated mice via the tail vein. Mice were sacrificed on day 3, and tumors were excised and immunostained. "T" indicates nests of tumor cells in tumor tissues. Bars represent 50 μm.

tumor patients. In fact, Avastin, the recombinant humanized monoclonal antibody against VEGF, has been widely used as an antiangiogenic drug, and its application range is spreading to the various types of solid tumors.[16] Other antiangiogenic proteins,[21,22] e.g., angiostatin, endostatin, and soluble forms of VEGF receptor, have also received great attention. Meanwhile, antiangiogenic gene therapy represents an attractive alternative to antiangiogenic proteins for reasons such as low dose, continuous expression of the therapeutic protein, and low cost. Therefore, development of an effective and safe gene vector is a key to successful antiangiogenic gene therapy.

In this study, thiolated PEG-PLys block copolymers were applied in the formation of disulfide cross-linked polyplex micelles for delivery of pDNA encoding sFlt-1, and tested for their antiangiogenic effect on mice bearing xenografted BxPC3 cell line, derived from human pancreatic adenocarcinoma. Disulfide cross-links in the polyplex core were designed to increase blood stability of the polyplex micelles and effectively release pDNA in the intracellular milieu.[10,11,18] PEG palisade of the polyplex micelle is expected to cover the polyplex core to shield the positive charge as well as to decrease interfacial free energy.[12,23] The formation of the PEG palisade surrounding the polyplex core was confirmed by the neutral zeta-potential of the polyplex micelles (Table 1). B-SH36% micelle showed an approximately 10 times higher concentration of pDNA in the blood at 60 min after iv injection than that of the micelle without core cross-linking

(B-SH0%) (Figure 4 in the Supporting Information). The disulfide cross-links in the polyplex core apparently contribute to the enhanced stability of the micelles in the bloodstream. Note that the size of polyplex micelles is between 100 and 150 nm (Table 1), which may be in a suitable range for accumulation in solid tumors due to the enhanced permeability and retention (EPR) effect,[24] although the size may be too large to allow the micelles to penetrate into the stroma in pancreatic tumors.[13] Nevertheless, there is a concern that excessive disulfide cross-links interfere with the smooth release of entrapped pDNA in the core, resulting in decreased transfection efficiency.[10] Accordingly, optimal cross-linking density should be determined to balance the stability and maintain high transfection efficiency. The results of *in vitro* real-time gene expression showed that B-SH5% micelle possessed the highest efficiency among the evaluated samples up to 60 h after transfection. It is noteworthy that B-SH11% micelle exerted sustained Luc expression and kept an appreciably high efficiency beyond 60 h (Figure 1). Apparently, gene expression is prolonged with an increase in cross-linking rates, although excess cross-links induced overstabilization of polyplex micelles, resulting in decreased transfection efficiency in the case of the B-SH20% and B-SH36% micelles. Eventually, the B-SH36%/sFlt-1 micelle had no *in vivo* efficiency, even though they showed the highest stability in the bloodstream among the evaluated samples (Figure 4 in the Supporting Information). It is also noteworthy that the B-SH11%/sFlt-1 micelle achieved an appreciably high therapeutic efficiency, even though it showed only limited improvement in blood circulation time compared to the B-SH0% and B-SH5% systems. Presumably, a sustained

(21) Sim, B. K. L.; MacDonald, N. J.; Gubish, E. R. Angiostatin and Endostatin: Endogenous Inhibitors of Tumor Growth. *Cancer Metastasis Rev.* **2000**, *19*, 181–190.

(22) Fischer, C.; Mazzone, M.; Jonckx, B.; Carmeliet, P. FLT1 and Its Ligands VEGFB and PlGF: Drug Targets for Anti-angiogenic Therapy. *Nat. Rev. Cancer* **2008**, *8*, 942–956.

(23) Kakizawa, Y.; Kataoka, K. Block Copolymer Micelles for Delivery of Gene and Related Compounds. *Adv. Drug Delivery Rev.* **2002**, *54*, 203–222.

(24) Matsumura, Y.; Maeda, H. A New Concept for Macromolecular Therapeutics in Cancer Chemotherapy: Mechanism of Tumoritropic Accumulation of Proteins and the Antitumor Agent Smancs. *Cancer Res.* **1986**, *46*, 6387–6392.

profile in gene expression may have been the key to this achievement. Note that no change in body weight of the mice was observed during the experiment (data not shown), indicating few serious side effects of polyplex micelles.

Comparison with the commercially available agents, gemcitabine and Avastin, confirmed the encouraging tumor growth suppression effect of the B-SH11% polyplex micelle (Figure 2b). Gemcitabine continues to be the standard therapy in the treatment of pancreatic tumors; however, its objective response rate is limited in patients with advanced disease.[25] Avastin is a recombinant humanized monoclonal antibody against human VEGF, which may neutralize tumor-cell-derived VEGF in the model used here. In humans, Avastin is the first clinically available antiangiogenic drug, and it has been efficient when used in combined chemotherapy for metastatic colorectal cancer[26] and non-small-cell lung cancer.[27] However, it showed no benefit in patients with pancreatic tumors.[25] The B-SH11%/sFlt-1 micelle significantly suppressed tumor growth compared not only to the control ($P < 0.001$) but also to the B-SH11%/Luc micelle, gemcitabine, and Avastin ($P < 0.01$) (Figure 2b). Xenografted BxPC3 was reported not to respond to gemcitabine,[28] probably due to its inability to penetrate through the tumor thick fibrotic tissue and target tumor cells, which is consistent with our results. Evaluation of vascular density in BxPC3 tumor (Figure 3) clearly showed that the B-SH11%/sFlt-1 micelle decreased vascular density compared to the control ($P < 0.001$), the B-SH11%/Luc micelle ($P < 0.001$), and Avastin ($P < 0.05$) treated tumors.

Inhibitory effect on tumor growth (Figure 2) is consistent with the result of decreased vascular density. There are several studies on antiangiogenic gene therapy for subcutaneously inoculated tumors in mice by systemic expression of sFlt-1 using viral vectors, including im injection of adeno-associated viral vectors[29] and iv injection of adenoviral vectors to target livers.[30] In these studies, however, sFlt-1 was expressed mainly in organs rather than tumor tissue.

What was worse, the excess expression of sFlt-1 in the liver led to unacceptable hepatotoxicity.[31] Thus, tumor-specific expression of sFlt-1 is essential for a safe and efficient antiangiogenic gene therapy. However, any nonviral gene vectors loading sFlt-1 gene have failed to exhibit selective gene expression in the tumor tissue, although they achieved certain inhibition of tumor growth.[8,9] In this regard, the B-SH11%/sFlt-1 micelle system might be promising, since sFlt-1 expression was significantly increased selectively in the tumor tissue compared not only to the control ($P < 0.001$) but also to the B-SH11%/Luc micelle ($P < 0.01$), as shown in Figure 4, without any significantly enhanced expression in other normal tissues. Note that no significant increase of sFlt-1 expression was observed in any normal organs treated with B-SH0%/sFlt-1 micelle or B-SH11%/Luc micelle. Histological analyses revealed that EGFP expression of the B-SH11%/EGFP micelle was located mainly around VECs but not in the tumor cells (Figure 5), probably due to restricted permeation of micelles by thick fibrotic tissues and pericyte-covered vasculature of the BxPC3 tumors. These results suggested the ability of expressed sFlt-1 molecule to entrap excess VEGF in the tumor tissue and to inhibit tumor growth by an antiangiogenic effect. Xenografted BxPC3 tumors in mice are characterized by stroma-rich histology,[20] which might explain the only slight inhibitory effects on BxPC3 growth achieved by gemecitabine[28] targeting tumor cells.

Conclusions

In conclusion, antiangiogenic gene therapeutic study was carried out by iv administration of polyplex micelles with sFlt-1 pDNA to mice bearing pancreatic adenocarcinoma BxPC3 xenografts, and the results demonstrated the ability of B-SH11% sFlt-1 micelle as a safe and effective gene delivery system. The optimal disulfide cross-linking rate of polyplex micelles was found to show significant suppression of tumor growth. Gene expression of sFlt-1 by iv injection of polyplex micelles was observed in tumor tissue only, followed by decreased vascular density and significant suppression of tumor growth. Based on these results, the B-SH11% disulfide cross-linked polyplex

(25) Rocha-Lima, C. M. New Directions in the Management of Advanced Pancreatic Cancer: a Review. *Anti-Cancer Drugs* **2008**, *19*, 435–446.

(26) Hurwitz, H.; Fehrenbacher, L.; Novotny, W.; Cartwright, T.; Hainsworth, J.; Heim, W.; Berlin, J.; Baron, A.; Griffing, S.; Holmgren, E.; Ferrara, N.; Fyfe, G.; Rogers, B.; Ross, R.; Kabbinavar, F. Bevacizumab Plus Irinotecan, Fluorouracil, and Leucovorin for Metastatic Colorectal Cancer. *N. Engl. J. Med.* **2004**, *350*, 2335–2342.

(27) Sandler, A.; Gray, R.; Perry, M. C.; Brahmer, J.; Schiller, J. H.; Dowlati, A.; Lilenbaum, R.; Johnson, D. H. Paclitaxel-carboplatin Alone or with Bevacizumab for Non-small-cell Lung Cancer. *N. Engl. J. Med.* **2006**, *355*, 2542–2550.

(28) Merriman, R. L.; Hertel, L. W.; Schultz, R. M.; Houghton, P. J.; Houghton, J. A.; Rutherford, P. G.; Tanzer, L. R.; Boder, G. B.; Grindey, G. B. Comparison of the Antitumor Activity of Gemcitabine and Ara-C in a Panel of Human Breast, Colon, Lung and Pancreatic Xenograft Models. *Invest. New Drugs* **1996**, *14*, 243–247.

(29) Takei, Y.; Mizukami, H.; Saga, Y.; Yoshimura, I.; Hasumi, Y.; Takayama, T.; Kohno, T.; Matsushita, T.; Okada, T.; Kume, A.; Suzuki, M.; Ozawa, K. Suppression of Ovarian Cancer by Muscle-Mediated Expression of Soluble VEGFR-1/Flt-1 Using Adeno-associated Virus Serotype 1-derived Vector. *Int. J. Cancer* **2006**, *120*, 278–284.

(30) Liu, J.; Li, J.; Su, C.; Huang, B.; Luo, S. Soluble Fms-like Tyrosine Kinase-1 Expression Inhibits the Growth of Multiple Myeloma in Nude Mice. *Acta Biochim. Biophys. Sin.* **2007**, *39*, 499–506.

(31) Mahasreshti, P. J.; Kataram, M.; Wang, M. H.; Stockard, C. R.; Grizzle, W. E.; Carey, D.; Siegal, G. P.; Haisma, H. J.; Alvarez, R. D.; Curiel, D. T. Intravenous Delivery of Adenovirus-mediated Soluble FLT-1 Results in Liver Toxicity. *Clin. Cancer Res.* **2003**, *9*, 2701–2710.